the discussion above and Eq. (26), the upper limit for the Fe^{2+} $\Delta M=1$ line is

$$\delta_D \approx \tfrac{2}{3}[7.32NB]; \quad (29)$$

and for the Ni^{2+} $\Delta M=2$ line,

$$\delta_D \approx \tfrac{2}{3}[9.06NB'], \quad (30)$$

where $B'=\gamma\gamma'/\hbar$. Here, γ refers to Ni^{2+} and γ' refers to Fe^{2+}.

The Fe^{2+} concentration in the crystals used was $2.0\times10^{18}/cm^3$. With this value and the γ, γ' given in reference 17, Eqs. (28), (29), and (30) yield the δ_D listed in Table II.

PHYSICAL REVIEW VOLUME 128, NUMBER 5 DECEMBER 1, 1962

Electron Drift Mobility in Silver Chloride*

R. VAN HEYNINGEN
Research Laboratories, Eastman Kodak Company, Rochester, New York
(Received July 30, 1962)

The drift mobility of electrons in silver chloride has been measured in the temperature range 70 to 350°K. In selected crystals, multiple trapping effects are not important, and the data represent the microscopic mobility. The experimental results are compared with existing theories of mobility in polar materials. It is suggested that the microscopic mobility is determined by the interaction of longitudinal optical phonons with polarons which have a temperature-dependent mass, and a temperature-dependent coupling between the electron and the lattice. The effect of multiple trapping at lower temperatures is shown, and the results are analyzed in terms of the concentration and energy depth of a single set of shallow trapping states.

I. INTRODUCTION

MEASUREMENTS of the drift and Hall mobilities of electrons in silver chloride have been reported by several authors.[1–4] The greatest success in fitting existing theories of electron mobility in polar materials[5–8] to the silver chloride data has been realized in a temperature range appreciably below the Debye temperature. The comparison of theory and experiment at higher temperatures, however, has been more uncertain because of the lack of sufficiently precise data in the temperature range above and including the Debye temperature.

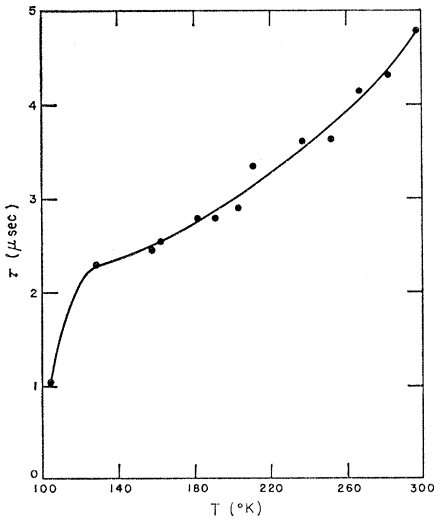

FIG. 1. Electron lifetime τ as a function of temperature in oxygen-doped AgCl, Sample C98–8.

The primary purpose of the present work was to clarify the experimental situation at higher temperatures, and thus provide a better check of available theories and for future theoretical work that may be more applicable to the case of silver chloride. Reproducible electron-mobility data, based on transit-time measurements, were obtained for a number of samples in the temperature range from 70 to 350°K. It was found that the available theories do not adequately describe the results.

II. EXPERIMENTAL

A. Electron Lifetime

Silver chloride is a wide bandgap photoconductor, and would, therefore, be an insulator in the dark were it not for its relatively large ionic conductivity. Impurity doping and mechanical strain affect the electronic as well as the ionic properties, and although these effects are not understood in detail, it is possible to prepare samples that have relatively long electron-trapping lifetimes (hereafter referred to simply as

* Communication No. 2311 from the Kodak Research Laboratories.

[1] J. R. Haynes and W. Shockley, Phys. Rev. **82**, 935 (1951).
[2] F. C. Brown and F. E. Dart, Phys. Rev. **108**, 281 (1957).
[3] K. Kobayashi and F. C. Brown, Phys. Rev. **113**, 508 (1959).
[4] L. Chollet and J. Rossel, Helv. Phys. Acta **33**, 627 (1960).
[5] D. Sowarth and E. Sondheimer, Proc. Roy. Soc. (London) **A219**, 53 (1953).
[6] R. L. Petritz and W. Scanlon, Phys. Rev. **97**, 1620 (1955).
[7] F. Low and D. Pines, Phys. Rev. **98**, 414 (1955).
[8] T. D. Schultz, Phys. Rev. **116**, 526 (1959).

lifetimes). The measurement of drift mobility by the transit-time technique requires that the electron lifetime be greater than the transit time which is typically of the order of 1 μsec in these experiments. Some ways to obtain samples in which the lifetime is longer than the transit time are discussed in the following paragraphs.

In well-annealed, nominally pure crystals containing a total of about one part per million of heavy-metal impurity ions,[9] the electron lifetime is usually of the order of 0.01 μsec at room temperature. The lifetime in the same material may be increased up to a maximum of about 10 μsec by doping with oxygen.[10] Figure 1 shows the temperature-dependence of the electron lifetime between 100 and 300°K in an oxygen-doped sample which was kept in the dark except for the small amount of light used in the measurements. The lifetime is relatively insensitive to temperature, which means that the density of effectively deep traps does not change much between 100 and 300°K in this material. For the present work, an electron trap is considered to be "deep" if the time for thermal generation of the electron from the trap into the conduction band is long compared to the time required to make a transient photocurrent measurement.

Recently, the silver halides have been successfully zone refined.[11] In the purest material, prepared in the absence of oxygen, the electron lifetime at room temperature is found to be relatively long. A maximum lifetime of 0.6 μsec has been observed.

Below about 200°K, the electron lifetime in most silver chloride crystals, whether they contain oxygen or not, can be increased greatly by exposure to light weakly absorbed in the fundamental absorption band. Filling of the traps by capture of electrons released by the light causes a decrease in the effective trap density, with a corresponding increase in the lifetime. When the traps are deep, the effective trap density may remain low for long times after the exposing light has been turned off. Recombination limited electron lifetimes up to 10 msec have been observed under these conditions. It has not been possible to measure hole currents, probably because of a low hole mobility.

Trap densities and trapping cross sections can be determined from measurements of the electron lifetime as a function of trap filling. If the trap density is N_t, and n of these are filled by capture of n electrons released by exposure in the fundamental absorption band, the lifetime is given by $\tau=1/(N_t-n)\sigma_t u$, where σ_t is the average trapping cross section and u is the thermal velocity. Both N_t and σ_t can be determined from two values of τ and n. At 100°K, in oxygen-doped crystals, it was found that the trap densities are low, $N_t\sim10^{12}$/cm^3, and the cross sections are large, $\sigma_t\sim10^{-13}$ cm^2.

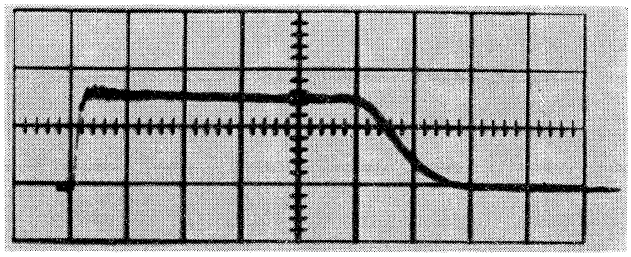

FIG. 2. Photocurrent–time waveform, showing electron transit across the crystal. Sample C98-9, $T=180$°K, sweep 1 μsec/cm.

Although the electron lifetime can be increased by exposure to light below about 200°K, above this temperature exposure leads to a decrease in the lifetime. This appears to be a result of a photochemical reaction between electronic and ionic charge carriers and defects,[12] such that the products of the reaction are electron traps either in higher density or with greater trapping cross sections than the traps present before the exposure.

B. Drift Mobility

Crystals with cross-sectional areas about 3 cm^2, and thicknesses from 2 to 5 mm were placed between plane-parallel transparent electrodes blocked with $\frac{1}{2}$-mil Mylar. Short-wavelength light, filtered from an air spark approximately 0.1 μsec in duration, was directed onto the sample through one of the electrodes. By using photoconductivity and optical absorption data, it was determined that the intensity and wavelength of the light were such that approximately 3×10^7 electron-hole pairs/cm^2 were released in an absorption depth of about 10^{-3} cm. The strongly absorbed light creates a sheet of free electrons and holes at the surface. Depending on the polarity of the applied field, a sheet of either free electrons or holes drifts toward the opposite electrode, while the carriers of the opposite sign are held at the blocked surface. The carriers that move across the crystal without being trapped (lifetime longer than the transit time) will be stopped at the opposite blocked electrode and the current associated with their motion will drop to zero. The time required for transit can be determined from the resulting current–time waveform, and the mobility can be obtained from the relation $\mu=l^2/VT$, where l is the sample thickness, V is the applied voltage, and T is the transit time.

At higher temperatures where ionic conduction is appreciable (above about 200°K), the motion of ionic charge carriers to the blocked electrodes causes the electric field in the sample to decrease with time after the voltage is applied. This difficulty was avoided experimentally by using a synchronized pulsed voltage

[9] N. Nail, F. Moser, P. E. Goddard, and F. Urbach, Rev. Sci. Instr. **28**, 275 (1957).
[10] F. C. Brown, J. Phys. Chem. Solids **4**, 206 (1958).
[11] F. Moser, D. C. Burnham, and H. H. Tippins, J. Appl. Phys. **32**, 48 (1961).
[12] F. Moser, N. Nail, and F. Urbach, J. Phys. Chem. Solids **9**, 217 (1959).

and delayed light-flash method similar in principle to that used by Brown.[10]

Figure 2 shows a current–time waveform obtained in the way just described. All determinations of the transit time were made from similar enlarged photographs. Because of the finite duration of the light flash, the electrons released at the cathode move away with a charge distribution in space related to the excitation function that describes the light flash. If this charge distribution did not change in transit, the current–time waveform would rise and fall symmetrically. In general, it does not, as can be seen in Fig. 2. The lengthening of the tail relative to the rise is attributed to a spreading of the charge distribution caused by diffusion and space charge within the sheet, and by multiple trapping.

The transit time was taken to be the time from the beginning of the current rise to the beginning of the fall, and as such corresponds to the motion of electrons at the leading edge of the charge distribution crossing the crystal. This determination of the transit time best avoids the inclusion of multiple-trapping effects in the data. When the transit time is plotted as a function of reciprocal applied voltage as in Fig. 3, it is seen that the dependence is essentially linear and extrapolates through the origin. The same dependence was observed for a number of samples at different temperatures. Consequently, it is assumed that this is a valid way to measure the transit time, and that the mobility is independent of the electric field strength in the range of field strengths used.

Figure 4 shows the temperature-dependence of electron drift mobility in four oxygen-doped samples, and one zone-refined sample prepared in the absence of oxygen. In all cases, at temperatures below about 200°K, the deep electron traps were filled by pre-exposure to weakly absorbed light before the measurements, so that the lifetimes were appreciably longer than the transit times. Sample C98–9 was the only sample in this set in which the electron lifetime above 200°K was long enough to get transit across the crystal in the applied field strengths used (maximum of 2000 V/cm). In this and other long-lifetime samples, the drift mobility was observed to drop rapidly with increasing temperature in the vicinity of 330°K, irreproducibly from sample to sample. This behavior appears to be structure-sensitive, and may be related to the rapidly increasing ionic conductivity. At lower temperatures the mobility may also be structure-sensitive, as shown by the data for Sample C98–14 in Fig. 4, curve 2, which will be discussed in Sec. III A. Mobility measurements on other samples showed a similar drop at low temperatures, caused by multiple trapping.

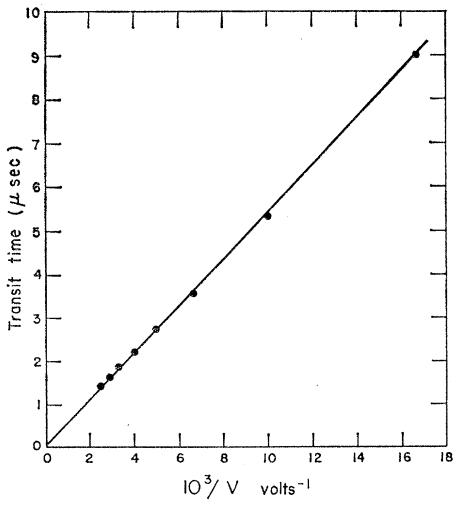

FIG. 3. Transit time T as a function of reciprocal applied voltage V. Sample C98–9, thickness $l=0.170$ cm, temperature 284°K, $\mu=l^2[dT/d(1/V)]^{-1}=54$ cm²/V-sec.

It is believed that the microscopic mobility is represented by curve 1 in Fig. 4 for the following reasons: The measurements never gave higher values of mobility than those shown in curve 1, but some samples did show mobilities lower than these as a result of multiple trapping. Maximum mobilities, apparently not affected by multiple trapping, were measured reproducibly from sample to sample, as shown by the data for curve 1. Furthermore, reported values of the Hall mobility[3] near 77°K, which is not affected by multiple trapping, are not greater than the values shown here; if anything, they are less.

The largest uncertainty in the values of mobility given here arises from the determination of the transit time. The relative values may be in error by about 5%, because of the inaccuracy in judging the transit time from the oscilloscope photographs. The absolute accuracy is affected principally by the definition of the transit time, which, as previously stated, was taken to be the time required for the leading edge of the charge distribution to cross the crystal. If the transit time is defined as the time required for the maximum of the charge distribution to cross the crystal, the resulting values of mobility are generally about 10% less than those given. Hence, it is reasonable to put limits of error on each point as +5% and −15%. The temperature was known to within less than one degree.

III. DISCUSSION OF RESULTS AND COMPARISON WITH THEORY

A. Drift Mobility with Multiple Trapping

For the case of a single electron-trapping level at an energy E below a spherical conduction band, and traps of concentration N_t, the drift mobility μ_d is related to the microscopic mobility μ_m by the expression[13]

$$\mu_d=\mu_m\frac{1}{1+(g_1/g_0)(N_t/N_c)\exp(E/kT)}, \qquad (1)$$

[13] F. C. Brown and K. Kobayashi, J. Phys. Chem. Solids 8, 300 (1959).

where N_c is the effective density of states near the bottom of the conduction band, and g_1 and g_0 are the statistical weights of the full and empty traps, respectively. For purposes of the present discussion, spin degeneracy is assumed so that $g_1/g_0=2$, and the effective mass m is taken to be $0.3m_e$. Then, $N_c=2(2\pi mkT/h^2)^{\frac{3}{2}}=7.9\times10^{14}T^{\frac{3}{2}}$.

The drift-mobility data of Fig. 4 can be analyzed by the use of Eq. (1). The data of curve 1 are taken to represent the microscopic mobility μ_m, and the points of curve 2 to represent a drift mobility μ_d reduced by multiple trapping at a single trapping level; E and N_t are determined unambiguously by values of μ_d/μ_m at two temperatures by Eq. (1) and found to be 0.02 eV and $5.7\times10^{14}/\text{cm}^3$, respectively. Curve 2 is a plot of μ_d as a function of reciprocal temperature using these values of E and N_t and the values of μ_m from curve 1. It is seen that the fit is very good. The identity of the centers responsible for this trapping has not been established. However, they are probably the same centers that have been observed to cause a peak in thermally stimulated current–temperature curves at 15°K.[14] Crystal C98–14 (data of curve 2) was cut from a cylindrical boule grown by the Bridgman technique[9] at a position midway between Samples C98–2 and C98–9. Since concentrations of impurities are found to vary uniformly with increasing concentrations toward the ends of the boule, and since neither C98–2 or C98–9 showed the effects of these traps, it seems unlikely that the multiple-trapping effects in Sample C98–14 are caused by simple chemical-impurity centers. It may be that they are associated with mechanical defects introduced by handling during the course of the experiment.

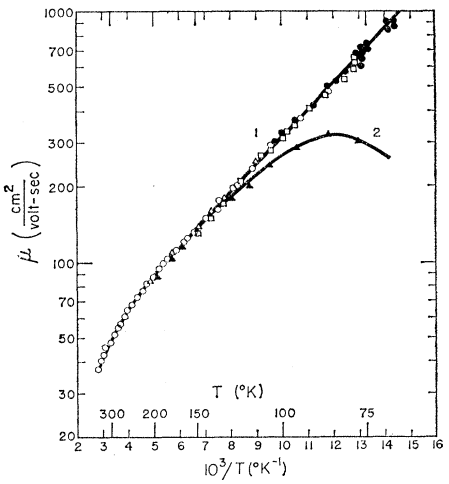

FIG. 4. Electron drift mobility as a function of reciprocal temperature. Curve 1 represents the microscopic mobility. Curve 2 shows the effects of multiple trapping at lower temperatures. Zone-refined, ● C106–3; oxygen-doped: △ C98–2, ○ C98–9, ▲ C98–14, □ C98–17.

B. Microscopic Mobility

Several theories have been developed for the scattering of electrons by the longitudinal optical modes of lattice vibrations in polar crystals. Low and Pines,[7] Feynman,[15] Schultz,[8] and others have considered the slow polaron problem, in which the polaron is defined as the electron with its associated cloud of lattice polarization. These theories are intended to be valid for values of the electron-lattice coupling constant α [see Eq. (5)] up to intermediate values of about 3 or 4, but the temperature is restricted to a range below the Debye temperature θ associated with the longitudinal optical modes of vibration, that is, $T\ll\theta$. The variational calculation of Howarth and Sondheimer[5] is not so restricted in temperature, but is valid only for $\alpha<1$. Furthermore, it is not a polaron theory. The reader is referred to the paper by Schultz for a careful comparison and criticism of the polaron theories, including the Schultz-Feynman theory, and to the article by Petritz and Scanlon[6] for a comparison of the Howarth-Sondheimer and Low-Pines theories. (Petritz and Scanlon have modified the Howarth-Sondheimer expression for the conductivity, and have used it to obtain an expression for the mobility. It should be noted that they use an older form of the Low-Pines theory in which a factor m/m^* is missing.) Silver chloride apparently has $\alpha\gtrsim2$[2,3,4,8] and a Debye temperature about 275°K. Consequently, the theoretical situation for silver chloride in the temperature range investigated, 70 to 350°K, is not very satisfactory.

All of the theoretical expressions involve the low-frequency dielectric constant, ϵ, and the Debye temperature, both of which are temperature-dependent. In what follows, the temperature-dependence of ϵ is taken from the work of Eucken and Büchner.[16] The Debye temperature of the longitudinal optical modes is given by $\theta=\hbar\omega/k$, where ω may be determined from the reststrahl frequency ω_t associated with the transverse optical modes by the relationship, $\omega=(\epsilon/\epsilon_0)^{1/2}\omega_t$.[17] Thus, ω contains the temperature-dependence of both ϵ and ω_t. Recently, Jones *et al.*[18] have measured ω_t in a number of materials. For AgBr they give the temperature-dependence between 4 and 300°K, and for AgCl the values at 4 and 300°K. For the present work, $\omega_t(T)$ for AgCl was obtained by interpolation by analogy with the AgBr data. The temperature-dependences of ϵ and θ have been plotted in Fig. 5. It is seen that θ varies from 258°K at $T=300$°K to $\theta=277$°K at $T=75$°K.

The Howarth-Sondheimer, Low-Pines, and Schultz-Feynman theories lead to the following expressions for

[14] R. Van Heyningen and F. C. Brown, Phys. Rev. **111**, 462 (1958).
[15] R. P. Feynman, Phys. Rev. **97**, 660 (1955).
[16] A. Eucken and A. Büchner, Z. physik. Chem. **B27**, 321 (1934).
[17] R. H. Lyddane, R. G. Sachs, and E. Teller, Phys. Rev. **59**, 673 (1941).
[18] G. O. Jones, D. H. Martin, P. A. Mawer, and C. H. Perry, Proc. Roy Soc. (London) **A261**, 10 (1961).

the mobility:

$$\mu_{\mathrm{HS}}=\frac{e}{2m\omega\alpha}\frac{8}{3\pi^{1/2}}\frac{\chi(Z)}{Z^{1/2}}(e^{\theta/T}-1), \tag{2}$$

where $\chi(Z)$ is a rather slowly varying function of $Z=\theta/T$.[5]

$$\mu_{\mathrm{LP}}=\frac{e}{2m\omega\alpha}\left(\frac{m}{m^*}\right)^3 f(\alpha)(e^{\theta/T}-1), \tag{3}$$

$f(\alpha)$ is a function of α approximately equal to one.[7]

$$\mu_{\mathrm{SF}}=\frac{e}{2m\omega\alpha}\left(\frac{m}{m^*}\right)\frac{v_r}{Z_r(2\hbar/m)^{1/2}}(e^{\theta/T}-1). \tag{4}$$

The parameter v_r is a resonance velocity, and Z_r is a coupling renormalization factor, both of which are functions of α.[8] α is given by

$$\alpha=\frac{e^2}{\hbar}\left(\frac{m_e}{2\hbar\omega}\right)^{1/2}\left(\frac{\epsilon-\epsilon_0}{\epsilon\epsilon_0}\right)\left(\frac{m}{m_e}\right)^{1/2}. \tag{5}$$

In these formulas, m_e represents the free electron mass; m, the effective mass that the electron would have in the static field of the crystal at rest; and m^*, the polaron mass. The ratios of the polaron to effective mass in the Low-Pines and Schultz-Feynman theories are given by

$$(m^*/m)_{\mathrm{LP}}=1+\tfrac{1}{6}\alpha, \tag{6}$$

and[4]

$$(m^*/m)_{\mathrm{SF}}=1+\tfrac{1}{6}\alpha+0.025\alpha^2+0.004\alpha^3. \tag{7}$$

Using the temperature-dependences of θ and ϵ, the theoretical temperature-dependence of the mobilities given by Eqs. (2), (3), and (4) are plotted in Fig. 6, together with the experimental curve. The theoretical curves have been normalized to the experimental data at 70°K, the lowest temperature at which measurements were made, and where the LP and SF theories in particular should be most valid. Using this normalization, values for α, m/m_e, m^*/m, and m^*/m_e were calculated

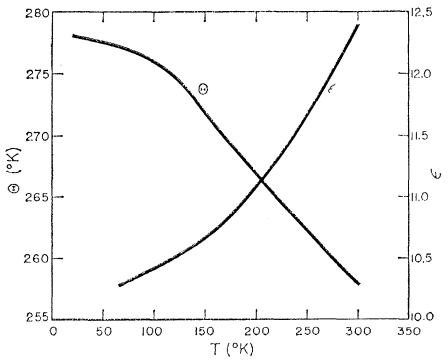

FIG. 5. The temperature-dependences of the low-frequency dielectric constant (Eucken and Büchner, reference 16), and the Debye temperature $\theta=(\hbar/k)(\epsilon/\epsilon_0)^{1/2}\omega_t$ (ω_t from Jones *et al.*, reference 18; see text).

TABLE I. Values of the mass ratios and the electron-lattice coupling constant α, determined by normalization of the theories to the experimental data at 70°K. The free electron mass is designated by m_e, the effective mass by m, and the polaron mass by m^*.

Theory	m/m_e	m^*/m	m^*/m_e	α
Howarth-Sondheimer	0.48	···	···	2.4
Schultz-Feynman	0.74	1.88	1.39	3.1
Low-Pines	0.31	1.33	0.41	2.00
Low-Pines-Yokota	0.29	1.30	0.38	1.93

and are given in Table I. The numbers are lower than most of the values previously reported.[2–4,8] This is a consequence of the fact that the mobility used in the calculations was higher than that given by the other workers.

If a straight-line extrapolation of the experimental $\log\mu$ vs $1/T$ curve is made to lower temperatures, it may be seen that all three of the theoretical curves cross it at the point chosen for normalization. As will be discussed later, such an extrapolation may not be valid. However, two things are to be noted. First, the values of α and the mass ratios are in error because of the arbitrariness of the normalization and the failure of theory to fit experiment. If the actual temperature-dependence should turn upward at lower temperatures and approach the theoretical temperature-dependence, a normalization of theory to experiment at the lower temperature would shift the theoretical curve downward in the temperature range shown here. As a result, the values of α and the mass ratios would be increased. Second, the theoretical curves have roughly the same slope, but are all steeper than the experimental curve. This is because the theoretical temperature-dependences are dominated by the phonon density factor $[e^{\theta/T}-1]^{-1}$. Since any theory is expected to include a phonon density term, this discrepancy in slope would remain unless other important factors were considered which depend rather strongly on temperature. There are at least two possibilities. Schultz[8] has pointed out that at high temperatures, the density of phonons effective for scattering may not vary simply as $[e^{\theta/T}-1]^{-1}$. Furthermore, the theories do not take into account a variation of the polaron mass with temperature, except insofar as α is temperature-dependent.

Yokota[19] has extended the Low-Pines theory to include a temperature-dependent polaron mass. For small α he gives

$$\left(\frac{m^*}{m}\right)_{\mathrm{Y}}=1+\frac{\alpha}{6(2\bar{n}+1)^{3/2}}, \tag{8}$$

where $\bar{n}=(e^{\theta/T}-1)^{-1}$. At low temperatures this reduces to the Low-Pines expression $(m^*/m)=1+\frac{1}{6}\alpha$. Osaka[20] has calculated, numerically, a temperature-dependence of the polaron mass using Feynman's formula-

[19] T. Yokota, Busseiron Kenkyu **69**, 137 (1953).
[20] Y. Osaka, Progr. Theoret. Phys. (Kyoto) **22**, 437 (1959).

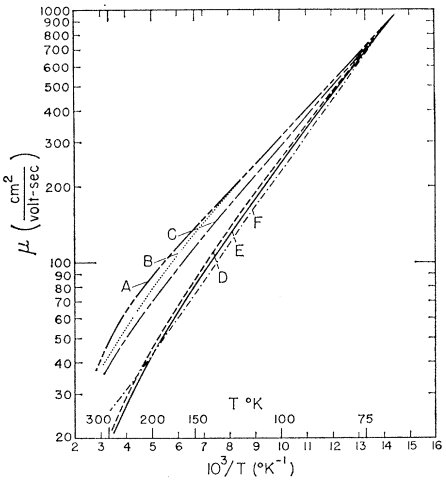

FIG. 6. Mobility as a function of reciprocal temperature: A: Experimental (same as curve 1 of Fig. 4); B: $[\exp(225/T)]-1$, $\theta=225°\text{K}=$constant; C: Low-Pines theory modified by Yokota's temperature-dependent polaron mass; D: Schultz-Feynman theory; E: Low-Pines theory; F: Howarth-Sondheimer theory.

tion[15] of the polaron problem for the case $\alpha=3$. His results are qualitatively similar to those of Yokota. In Fig. 6, curve C is a plot of the Low-Pines theory modified by Eq. (8), and is again normalized at 70°K. The use of Eq. (8) instead of Eq. (6) leads to slightly different values of α, m/m_e, and m^*/m_e, as given in Table I. Curve C shows that the inclusion of the temperature-dependence of the polaron mass brings theory closer to experiment. Below 70°K, $(m^*/m)_Y$ and $m^*/m)_{LP}$ are essentially identical, but above 70°K there is an increasingly greater and significant difference. For example, the relative values of mobility are changed by 1.03, 1.14, 1.57, and 1.83, at the temperatures 70, 100, 200, and 300°K, respectively. The result is that the slope of the theoretical curve is not as great at higher temperatures. Qualitatively, Osaka's results used with the Schultz-Feynman mobility expression show the same effect, but it is not as pronounced, since m/m^* enters only as the first power instead of the third, as in the Low-Pines theory.

The preceding discussion may mean that an extrapolation of the present data to lower temperatures, as discussed earlier, is questionable, that is, the temperature-dependence may be relatively steeper at lower temperatures. Recent Hall mobility measurements on AgCl at lower temperatures by Masumi and Brown[21] show that the temperature-dependence can be fitted quite well by $e^{284/T}-1$, which is steeper than the temperature-dependence reported here in the range of $200°\text{K}>T>70°\text{K}$. Masumi and Brown's results are consistent with theory, in that θ is essentially constant and equal to approximately 280°K at temperatures below 70°K.

It has been assumed that the values used for θ are substantially correct, and that the Debye temperature determined in the way described is applicable to this problem. However, one may take the point of view that the effective Debye temperature should be determined from the mobility data. On assuming a constant θ and a temperature-dependence of the form $(\exp\theta/T)-1$, the best fit is obtained with $\theta=225°\text{K}$; $\mu_0[(\exp\theta/T)-1]$ is shown as curve B in Fig. 6. The use of this value of θ would, of course, change the values of α and the mass ratios, and would not be consistent with the lower temperature results of Masumi and Brown.[21]

Curve A, Fig. 6, shows that, above 200°K, the experimentally determined mobility falls below the straight-line extrapolation of the lower temperature data to higher temperatures. The theoretical curves also show a similar drop, with the exception of curve F, plotted from the Howarth-Sondheimer theory. The main reason for the drop in the theoretical mobility at higher temperatures is the increasing importance of the -1 in the term $(\exp\theta/T)-1$, for temperatures in the vicinity of, and above, the Debye temperature. A smaller, but not insignificant, contribution to the drop is the increase of α with increasing temperature. Figure 7 is a plot of relative values of α vs reciprocal temperature, calculated from Eq. (5), using temperature-dependent values of ω and ϵ. Comparison of Figs. 6 and 7 shows that α increases with temperature in a manner analogous to the decrease of mobility with increasing temperature. A decrease in the mobility is expected with an increasingly strong coupling of the electron with the lattice. This may also be seen by an inspection of Eqs. (2)–(4), each of which has α at least to the negative first power, and in Eqs. (3) and (4), reciprocals of polynomials in α through m/m^*. Hence, in terms of the theories, the

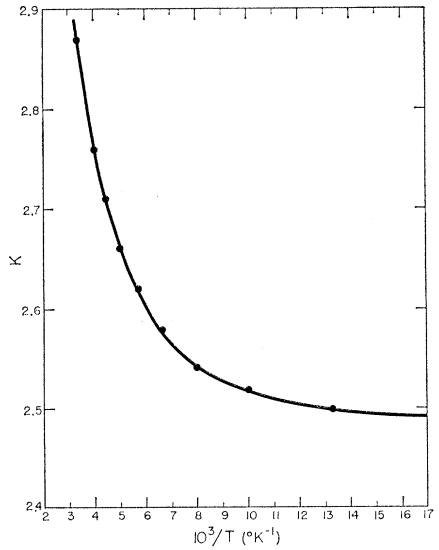

FIG. 7. Relative values of the electron-lattice coupling constant as a function of reciprocal temperature. The ordinate K is defined by

$$K(T)=\alpha\Big/\frac{e^2}{\hbar}\Big(\frac{m_e}{2\hbar}\frac{m}{m_e}\Big)^{1/2}=\frac{1}{\omega^{1/2}}\Big(\frac{\epsilon-\epsilon_0}{\epsilon\epsilon_0}\Big).$$

[21] T. Masumi and F. C. Brown (to be published).

relative dropping off of the mobility at higher temperatures may be attributed to a rapidly increasing phonon density, $1/(e^{\theta/T}-1)$, and an increasing electron-lattice coupling constant α.

IV. CONCLUSIONS

Currently available theories of electron mobility in polar materials have been formulated with assumptions that limit their applicability to silver chloride in the temperature range studied. The comparison of the theories with the data shows, as might be expected, that the theories do not adequately describe the results. However, the best fit of theory to experiment suggests that the mobility and its temperature-dependence may be interpreted in terms of longitudinal optical mode scattering of polarons which have a temperature-dependent mass, and a temperature-dependent coupling between the electron and the lattice.

ACKNOWLEDGMENTS

The author is indebted to Professor F. C. Brown, Dr. D. C. Hoesterey, Dr. F. Garcia-Molinar, and Professor D. L. Dexter for helpful suggestions and discussions during the course of this work. He also wishes to acknowledge the cooperation of, and interesting discussions with, Dr. F. Urbach, Dr. D. C. Burnham, and F. Moser who also provided the silver chloride crystals.

PHYSICAL REVIEW VOLUME 128, NUMBER 5 DECEMBER 1, 1962

Antiferromagnetism of the Antiphase Domain Structure of Pd_3Mn

J. W. CABLE, E. O. WOLLAN, W. C. KOEHLER, AND H. R. CHILD
Oak Ridge National Laboratory, Oak Ridge, Tennessee

(Received July 16, 1962)

Neutron diffraction measurements were made on polycrystalline samples of a 75% Pd−25% Mn alloy. It was found that long-range positional order could be obtained by appropriate heat treatment and that this order was of the one-dimensional antiphase domain type with a period of 4 cubic unit cells. Below 170°K antiferromagnetic reflections were observed for this ordered alloy. A magnetic structure is proposed which satisfactorily accounts for the observed magnetic reflection intensities. On the basis of this structure the atomic magnetic moments are $(4.0\pm0.2)\mu_B$/Mn and $(0.2\pm0.1)\mu_B$/Pd.

THE paramagnetic behavior of pure palladium is appreciably altered by the addition of small amounts of the 3*d* metals. Addition of iron or cobalt leads to ferromagnetism[1–4] while alloying with chromium or manganese increases the antiferromagnetic tendencies of the system.[4–6] This investigation of Pd_3Mn was undertaken as part of a general neutron diffraction program inquiring into the existence of localized magnetic moments on the palladium atoms and the participation of these atoms in the magnetic exchange interactions of these alloy systems.[7–9]

For this study long-range antiferromagnetic order was necessary and it was considered most likely that this would occur in a positionally ordered alloy. In addition, it was felt that positional order would most likely occur for an alloy in the 3 to 1 composition region. Accordingly, an alloy containing 25 at.% manganese was prepared. The arc melted sample was filed to an 80-mesh powder and heat treated by cooling from 1000°C to room temperature over a period of 2 weeks. Neutron diffraction data were taken before and after the heat treatment and typical patterns are shown in Fig. 1. In the lower part of the figure is the pattern obtained before heat treatment and only the normal lattice reflections for the face-centered cubic structure appear. The corresponding disordered structure is depicted on the right of the pattern where the random distribution of the two types of atoms on the lattice sites is represented by an average atom at each site. The pattern obtained for the heat treated sample is shown in the upper part of the figure and long-range positional order is indicated by the intense superlattice reflections. The reflections were indexed on the basis of the cell shown at the right of the pattern. This is a one-dimensional antiphase domain structure based on the Cu_3Au type of order. The antiphase domain boundaries, which occur in two unit cell intervals, are perpendicular to the a_3 axis and are characterized by atomic displacements of $(a_1+a_2)/2$. The intensities calculated for this model

[1] J. Burger and J. Wucher, Compt. rend. **245**, 2230 (1957).
[2] J. Crangle, Phil. Mag. **5**, 335 (1958).
[3] R. M. Bozorth, P. A. Wolff, D. D. Davis, V. B. Compton, and J. H. Wernick, Phys. Rev. **122**, 1157 (1960).
[4] D. Gerstenberg, Ann. Phys. (New York) **2**, 236 (1958).
[5] J. Wucher, *Colloque National de Magnetisme* (Centre National de la Recherche Scientifique, 1958), p. 139.
[6] J. Burger and J. Wucher, Compt. rend. **251**, 2667 (1960).
[7] E. O. Wollan, Phys. Rev. **122**, 1710 (1961).
[8] E. O. Wollan, J. W. Cable, W. C. Koehler, and M. K. Wilkinson, J. Phys. Soc. Japan (to be published).
[9] J. W. Cable, E. O. Wollan, W. C. Koehler, and M. K. Wilkinson, Suppl. J. Appl. Phys. **33**, 1340 (1962).

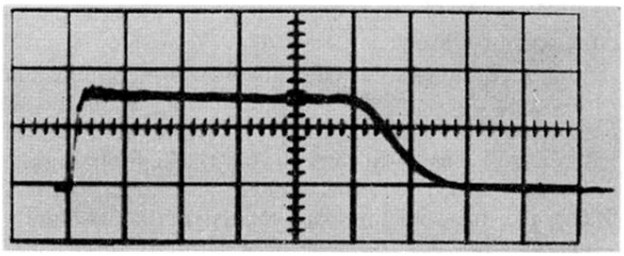

FIG. 2. Photocurrent–time waveform, showing electron transit across the crystal. Sample C98–9, $T = 180°K$, sweep 1 μsec/cm.